



## Synthesis of Nanocellulose Facilitated by Ionic Liquid using *Pongamia pinnata* as Biomass Resource

H.K. PRADEEP\*<sup>ORCID</sup> and DIPTI H. PATEL<sup>ORCID</sup>

Department of Pharmaceutics, Institute of Pharmaceutical Sciences, Faculty of Pharmacy, Parul University, P.O. Limda, Tal. Waghodia-391760, India

\*Corresponding author: E-mail: pradeepkmgmips@gmail.com

Received: 12 June 2024;

Accepted: 17 July 2024;

Published online: 30 August 2024;

AJC-21733

The successful transformation of cellulose into nanocellulose was conducted from *Pongamia pinnata* utilizing ionic liquid, 1-butyl-3-imidazolium chloride, as a swelling agent and catalyst. The SEM analysis revealed the presence of a fibrillar structure, disordered agglomerates, highly organized and smooth nanofibers. The studies confirmed the presence of thread-like structures and the existence of strong intermolecular linkages as that of cellulose. The X-ray diffraction (XRD) study and thermogravimetric analysis (TGA) demonstrated that the semicrystalline nature of nanocellulose retained and exhibited stable thermal characteristics. The utilization of 1-butyl-3-imidazolium chloride as a catalyst and swelling agent has presented an efficient and eco-friendly approach for the synthesis of nanocellulose.

**Keywords:** Ionic liquid, Nanocellulose, *Pongamia pinnata*.

### INTRODUCTION

Cellulose is a type of linear polysaccharide consisted of hydrogen-bonded repeating units of  $\beta$ -1-4-linked D-glucopyranose which form six-membered rings [1]. It has found extensive application as a building material and energy source due to its non-toxic, biodegradable, and biocompatible properties. However, the intractable nature of cellulose in water and typical organic solvents restricts its ability to be functioning in the aqueous phase. Nanocellulose refers to cellulose particles that are on a nanoscale and have the ability to create a consistent and stable suspension when suspended in water [2,3].

Lignin, hemicellulose and cellulose are the constituents of lignocellulosic biomass. Nanocellulose is derived from cellulose, which is obtained from processed lignocellulosic material through an alkali treatment that removes the lignin. Both mechanical and chemical methods can be employed to produce nanocellulose from cellulose. The mechanical method consists of enhanced ultrasonication or high-pressure homogenization, while the chemical process incorporates acid hydrolysis, ionic liquid and 2,2,6,6-tetramethylpiperidine-1-oxyl (TMPO) agent [4-7].

Ionic liquids (ILs), a novel category of environmentally friendly solvents or agents for swelling, are being regarded as

an optimal substitute for extracting cellulose nanowhiskers from cellulosic matrix using milder conditions [8]. Ionic liquids has distinctive characteristics, including low toxicity, non-flammability, recyclability and strong chemical and thermal stabilities. These properties make ionic liquids a viable medium for separating nanocellulose from cellulosic sources.

Ionic liquids (ILs) can function as catalysts in the process of cellulose hydrolysis, resulting in the production of high-crystallinity cellulose nanocrystals (CNC). The imidazole ionic liquids containing  $\text{HSO}_4^-$  or  $\text{Cl}^-$  anion, such as 1-butyl-3-methylimidazolium hydrogen sulphate ([Bmim]HSO<sub>4</sub>) and 1-butyl-3-methylimidazolium chloride ([Bmim]Cl), have been identified as the most appropriate options for this specific application. Tan *et al.* [9] employed [Bmim]HSO<sub>4</sub> as both a catalyst and solvent to enzymatically esterify and generate CNC. The facile one-pot approach was uncomplicated and ecologically sound. Iskak *et al.* [10] demonstrated that the CNC properties were improved when the reaction temperature and time increased. Using ionic liquid at moderate temperatures and without strong chemicals, cellulose can be transformed into nanocellulose while retaining its original structure. Moreover, ionic liquid efficiently removes the amorphous cellulose, hemicellulose and lignin from the cellulose structure, resulting in the production of high-quality nanocellulose. By considering the solubility properties

of various types of ionic liquids, it is feasible to control the dimensions and the structure of nanocellulose. Several ionic liquids possess the ability to be recycled and reused, hence improving the sustainability of the process [11,12].

In this work, an approach is used to synthesize nanocellulose from the lignocellulosic mass of *Pongamia pinnata* using 1-butyl-3-methylimidazolium chloride as a swelling agent and catalyst. The obtained product was characterized by FTIR, XRD, SEM and TGA/DTA techniques.

## EXPERIMENTAL

The lignocellulosic materials of *Pongamia pinnata* husk were obtained locally from saw mills located in Davanagere city, India. The chemicals, namely 1-butyl-3-methylimidazolium chloride ([BMIm][Cl]), sodium hypochlorite, sodium hydroxide, acetic acid and sodium chlorite were procured from SD Fine Chem Pvt. Ltd. India. All chemicals were of a highest purity and utilized without further any purification.

**Extraction of cellulose from *Pongamia pinnata*:** The fine husk of *Pongamia pinnata* was passed through sieve number 44 with an aperture size of 355  $\mu\text{m}$  to obtain a moderately fine powder and then stored in an airtight container. About 25 g of moderately fine powder was delignified by treating it with 5% w/v NaOH at 60–70 °C and then dried overnight. Dried delignified mass was then bleached using 5% w/v NaClO<sub>2</sub> (sodium chlorite), to which 3 mL of acetic acid solution was added. Throughout the bleaching process, a temperature of 70 °C was maintained to obtain the cellulose [13].

**Synthesis of nanocellulose:** The nanocellulose was synthesized by pouring 10 g of [Bmim]Cl into a 100 mL dry two-necked flask. The flask was fitted with a water-cooled condenser and a calcium guard tube at the outlet and then placed in an oil bath. Then, 1 g of dehydrated and finely pulverized *Pongamia pinnata* cellulose was separately and gradually introduced into the flask containing the ionic liquid. The mixture was then heated and stirred using a thermomagnetic stirrer at 115–120 °C for 1–2 h. After dissolution, a pale yellow solution was formed and then diluted by adding 50 mL of ice-cold distilled water. The precipitated nanocellulose was filtered and subjected to 5–6 times of washing with cold distilled water. Subsequently, it was treated with ultrasonication for 45 min, centrifuged at 2000 rpm for 30 min, then the reaction material was dehydrated and preserved.

**Characterization:** The infrared spectra of *P. pinnata* cellulose and ionic liquid treated *P. pinnata* nanocellulose (PILN) samples were measured in the range of 4000–400  $\text{cm}^{-1}$  using a Bruker ATR alpha instrument at  $25 \pm 0.5$  °C to identify the functional groups. The XRD data was recorded by using a Make Rigaku, Model Smart Lab Diffractometer within a scanning angle range of 10–80° and a scanning speed of 0.18°  $\text{min}^{-1}$ . The NETZSCH STA 2500 was used for TGA/DTA analysis in the temperature range of 30 to 900 °C/min. The SEM images were obtained from Hitachi SU 3500 instrument operated at an accelerating voltage of 10 kV and evaluated at various magnifications including 60X, 200X and 500X. 1.10X and 2.50X.

## RESULTS AND DISCUSSION

**FTIR studies:** Fig. 1 illustrates the spectral analysis of cellulose and nanocellulose indicating the existence of similar functional groups. The cellulose and nanocellulose obtained from ionic liquid were subjected to spectral analysis, which revealed a distinct peak at 3325–3315  $\text{cm}^{-1}$ . This peak can be attributed to the existence of -OH groups, possibly due to the intermolecular hydrogen bonding. The presence of the bending mode of the adsorbed water is shown by the vibrational peak within the range of 1635–1625  $\text{cm}^{-1}$ . The peaks identified in the cellulose spectrum, within the range of 1203  $\text{cm}^{-1}$ , can be ascribed to the elongation of the carbon-oxygen (C-O) bonds and the oscillation of the carbon-hydrogen (C-H) bonds. The peak at approximately 826  $\text{cm}^{-1}$ , which is believed to be due to the  $\beta$ -glycosidic linkage, was assigned to the stretching of the O-C-O bond while the C-H bonds in cellulose were observed at 1046  $\text{cm}^{-1}$ .

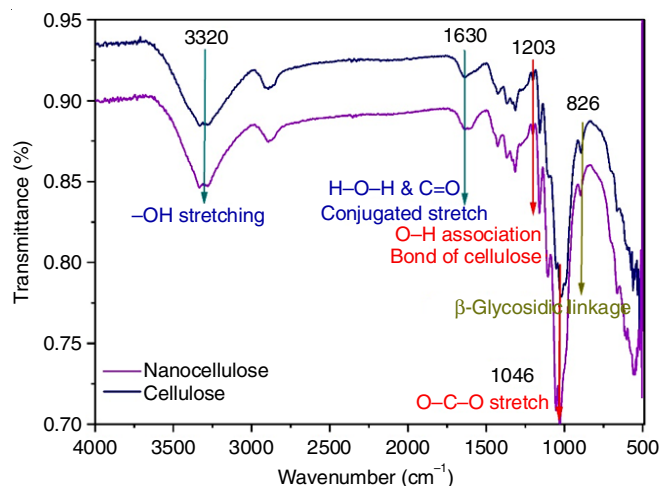


Fig. 1. Comparative FTIR between cellulose and nanocellulose obtained from ionic liquid method

**XRD studies:** The sharp peaks at 22.5° and 26.48° are the indicative of well-ordered crystalline regions, while the broad peak at 16.03° suggests the presence of amorphous content as shown in Fig. 2. This information is crucial for understanding the material properties of nanocellulose, as the crystalline regions contribute to its strength and rigidity, while the amorphous regions may influence its flexibility.

**Thermal studies:** The onset temperature is a crucial characteristic that indicates the thermal stability of the nanocellulose. As shown in Fig. 3 at 289.6 °C, the nanocellulose undergoes decomposition. The observed temperature indicates the initiation of substantial heat deterioration in nanocellulose, potentially caused by the breakdown of the cellulosic polymer chains at  $\beta$ -glycosidic linkages leading to formation of volatile products like water, carbon dioxide and organic compounds. At 359 °C, nanocellulose reaches the end of the primary the decomposition phase. At this stage, most of the nanocellulose has undergone decomposition as evidenced by a significant decrease in mass of 89.72%. The residual mass accounts for just a small proportion of the starting mass, which could be composed of thermally stable components that do not evaporate

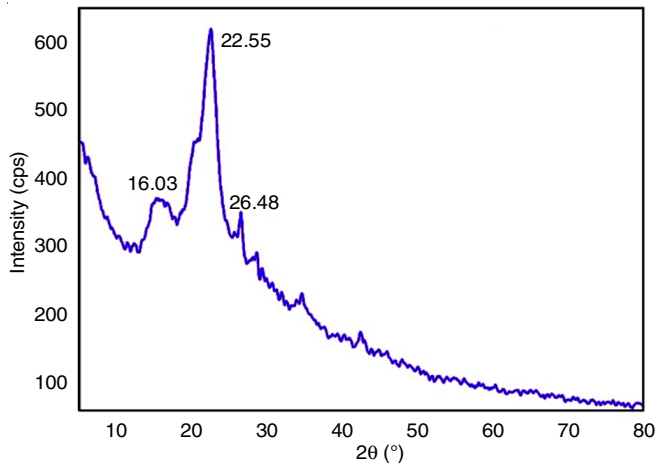


Fig. 2. XRD spectrum of *Pongamia pinnata* nanocellulose

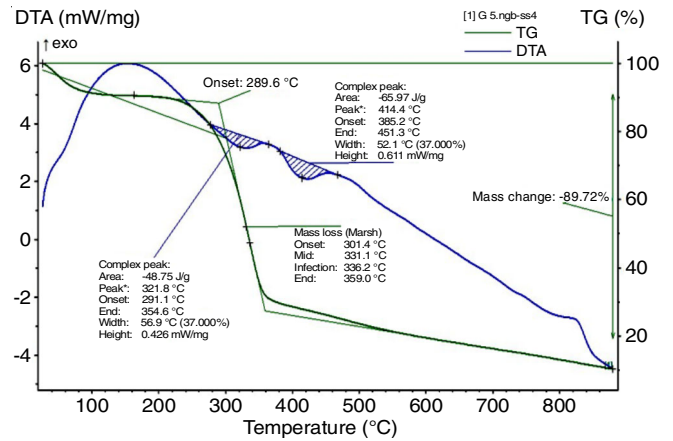


Fig. 3. TGA/DTA thermogram of *Pongamia pinnata* nanocellulose

under the testing conditions. Based on these results nanocellulose obtained by ionic liquid thermally stable upto 289.6 °C.

**DTA:** A significant heat impact within the nanocellulose structure is indicated by the initial endothermic peak that occurs between 291 °C and 354.6 °C, with a maximum at 321.8 °C and an enthalpy change of -48.75 J/g. This occurrence can be

assigned to the heat degradation or depolymerization of the cellulose chains. Thermal break down of nanocellulose usually starts within this temperature range. The breakdown of glycosidic linkages in the cellulose polymer chains, which breaks them into smaller molecular pieces and releases volatile components, is directly proportional to the energy absorbed throughout the process. This peak may also suggest the depolymerization

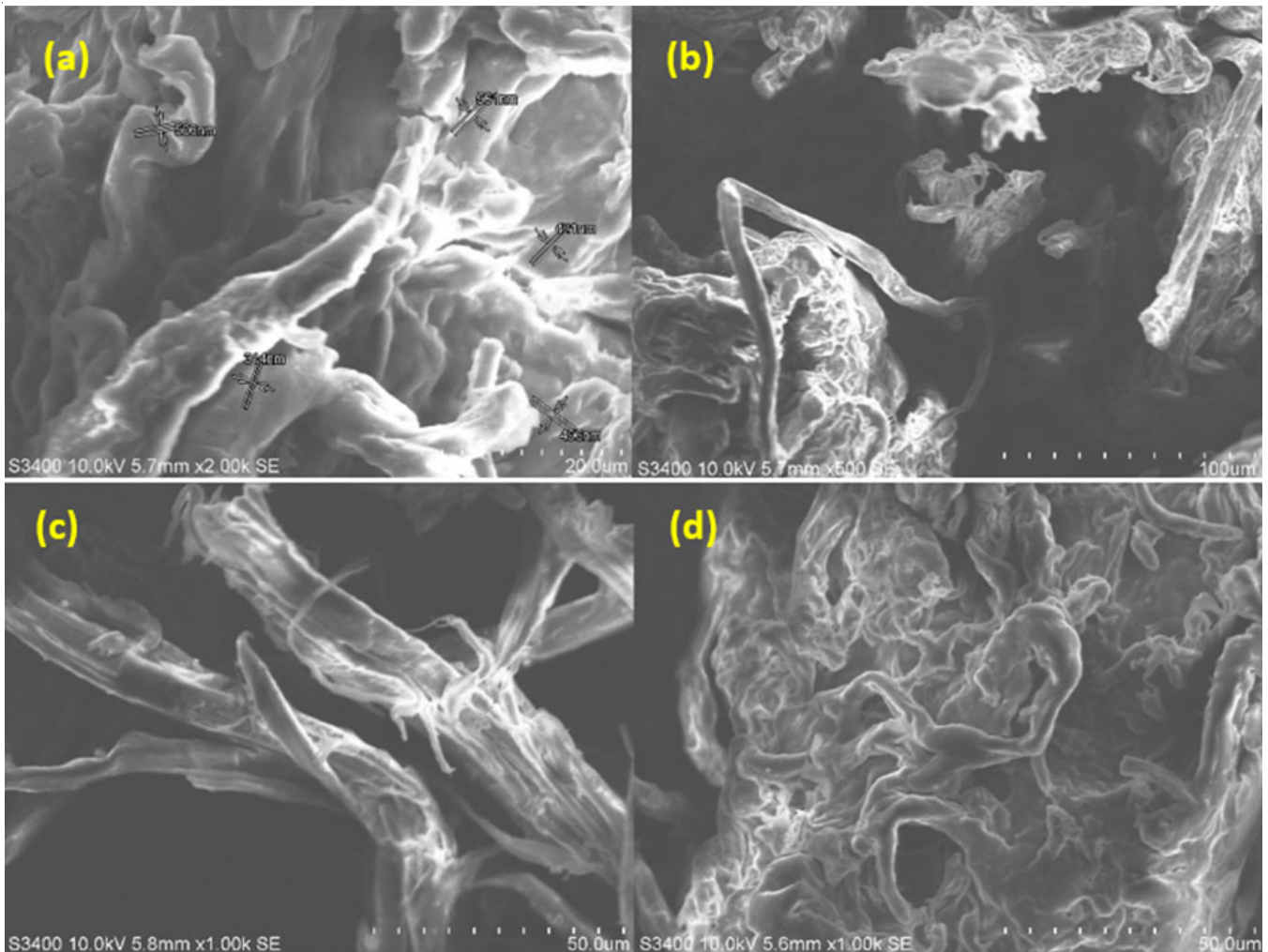


Fig. 4. SEM images of *Pongamia pinnata* nanocellulose

process, in which the lengthy cellulose chains disintegrate into smaller units. According to the enthalpy change, the structural integrity of the nanocellulose significantly decreases within this temperature range. As shown in Fig. 3, the thermal degradation process reaches its maximum rate at the temperature where the energy absorption is significant, which is 321.8 °C. The second endothermic peak, observed within the temperature range of 385.2 °C and 451.3 °C, with the highest point at 414.4 °C and a corresponding enthalpy change of -65.97 J/g, indicates another significant thermal occurrence, potentially linked to more decomposition or alterations in the material's phase. The presence of this elevated temperature endothermic peak indicates more degradation of the nanocellulose substance. At this point, the cellulose may be undergoing decomposition into smaller, volatile molecules, gasses and carbonaceous leftovers. A higher enthalpy change signifies a process that requires more energy, which aligns with the total disintegration of cellulose structure.

**SEM studies:** According to the SEM images (Fig. 4), the structure of the synthesized nanocellulose was found to disordered agglomerates and nanofibers were found highly ordered and smooth. The ionic liquid oriented nanocellulose synthesis revealed the presence of microfibers of nanocellulose, which exhibited thread-like architectures and demonstrated robust intermolecular interactions [14]. The smooth surface of nanocellulose is the advantage for the biomedical applications [15] and the size of the nanofibers were in the range 300–600 nm fibers with voids forming uneven surface.

## Conclusion

This study exploited a type of agricultural biomass obtained from *P. pinnata* to produce nanocellulose through ionic liquid. The FTIR analysis of cellulose in lignocellulosic biomass revealed peaks in the nanocellulose, indicating that there were no aberrations in reactions during the process of degrading cellulose into nanocellulose. X-ray crystallographic studies have shown that produced nanocellulose displays a semicrystalline nature, characterized by amorphous broad humps and sharp peaks. During the entire process, the disruption of hydrogen bonds in cellulose caused the dissolution of its crystalline nature. The SEM pictures revealed various shapes with an uneven surface, consistent cross-sections and a large quantity of microscopic microfibrils. Based on TGA/DTA analysis, the presence of pronounced dips in the curve indicated that the point at which the breakdown of cellulose treated with ionic liquid begins is approximately 289.6 °C. Furthermore, the treated cellulose exhibited enhanced resistance to high temperatures. Moreover, this study seeks to illustrate the impressive practical uses of artificially

produced nanocellulose derived from agricultural biomass. This will undoubtedly address India's requirement for effective biopolymer usage in pharmaceuticals, drug delivery, tissue engineering, and various industrial applications, water purification, sensor application adopting a more practical approach to nanocellulose production.

## CONFLICT OF INTEREST

The authors declare that there is no conflict of interests regarding the publication of this article.

## REFERENCES

1. P.H. Keshavamurthysetty and D.H. Patel, *Indian J. Pharm. Educ. Res.*, **57(1s)**, s32 (2023); <https://doi.org/10.5530/ijper.57.1s.5>
2. R.H. Atalla and D.L. VanderHart, *Science*, **223**, 223 (1984); <https://doi.org/10.1126/science.223.4633.283>
3. H. Kobayashi, Y. Ito, T. Komanoya, Y. Hosaka, P.L. Dhepe, K. Kasai, K. Hara and A. Fukuoka, *Green Chem.*, **13**, 326 (2011); <https://doi.org/10.1039/C0GC00666A>
4. L. Feng and Z. Chen, *J. Mol. Liq.*, **142**, 1 (2008); <https://doi.org/10.1016/j.molliq.2008.06.007>
5. J.K. Prasannakumar, G.K. Prakash, H.S. Onkarappa, B. Suresh and B.E. Basavarajappa, *Asian J. Chem.*, **34**, 2639 (2022); <https://doi.org/10.14233/ajchem.2022.23900>
6. N. Lin and A. Dufresne, *Eur. Polym. J.*, **59**, 302 (2014); <https://doi.org/10.1016/j.eurpolymj.2014.07.025>
7. P. Jagadesh, A. Ramachandramurthy and R. Murugesan, *Constr. Build. Mater.*, **176**, 608 (2018); <https://doi.org/10.1016/j.conbuildmat.2018.05.037>
8. S. Mahmoudian, M.U. Wahit, A.F. Ismail and A.A. Yussuf, *Carbohydr. Polym.*, **88**, 1251 (2012); <https://doi.org/10.1016/j.carbpol.2012.01.088>
9. X.Y. Tan, S.B. Abd Hamid and C.W. Lai, *Biomass Bioenergy*, **81**, 584 (2015); <https://doi.org/10.1016/j.biombioe.2015.08.016>
10. N.A.M. Iskak, N.M. Julkapli and S.B.A. Hamid, *Cellulose*, **24**, 2469 (2017); <https://doi.org/10.1007/s10570-017-1273-2>
11. A.S. Norfarhana, R.A. Ilyas, N. Ngadi and M.H. Dzarfan Othman, *Heliyon*, **10**, e27715 (2024); <https://doi.org/10.1016/j.heliyon.2024.e27715>
12. A.A. Shamsuri, S.N.A. Md. Jamil and K. Abdan, *Front. Mater.*, **9**, 919918 (2022); <https://doi.org/10.3389/fmats.2022.919918>
13. J.K. Prasannakumar, G.K. Prakash, B. Suresh, B.E. Basavarajappa, H.S. Onkarappa, B.K. Devendra and S.G. Prasannakumar, *Asian J. Chem.*, **35**, 83 (2023); <https://doi.org/10.14233/ajchem.2023.23999>
14. D.M. Panaitescu, S. Vizireanu, C.A. Nicolae, A.N. Frone, A. Casarica, L.G. Carpen and G. Dinescu, *Nanomaterials*, **8**, 467 (2018); <https://doi.org/10.3390/nano8070467>
15. E.C. Lengowski, E.A. Bonfatti Júnior, L. Simon, G.I.B. de Muñiz, A.S. de Andrade, S. Nisgoski and U. Klock, *Cellulose*, **27**, 10855 (2020); <https://doi.org/10.1007/s10570-020-03232-4>